



Measurement of the branching fraction of the $B^0 \rightarrow K_s^0 \pi^0 \gamma$ decay using 190 fb^{-1} of Belle II data

Belle II Collaboration: F. Abudinén, I. Adachi, K. Adamczyk, L. Aggarwal, P. Ahlburg, H. Ahmed, J. K. Ahn, H. Aihara, N. Akopov, A. Aloisio, F. Ameli, L. Andricek, N. Anh Ky, D. M. Asner, H. Atmacan, V. Aulchenko, T. Aushev, V. Aushev, T. Aziz, V. Babu, S. Bacher, H. Bae, S. Baehr, S. Bahinipati, A. M. Bakich, P. Bambade, Sw. Banerjee, S. Bansal, M. Barrett, G. Batignani, J. Baudot, M. Bauer, A. Baur, A. Beaubien, A. Beaulieu, J. Becker, P. K. Behera, J. V. Bennett, E. Bernieri, F. U. Bernlochner, V. Bertacchi, M. Bertemes, E. Bertholet, M. Bessner, S. Bettarini, V. Bhardwaj, B. Bhuyan, F. Bianchi, T. Bilka, S. Bilokin, D. Biswas, A. Bobrov, D. Bodrov, A. Bolz, A. Bondar, G. Bonvicini, A. Bozek, M. Bračko, P. Branchini, N. Braun, R. A. Briere, T. E. Browder, D. N. Brown, A. Budano, L. Burnistrov, S. Bussino, M. Campajola, L. Cao, G. Casarosa, C. Cecchi, D. Červenkov, M.-C. Chang, P. Chang, R. Cheaib, P. Cheema, V. Chekelian, C. Chen, Y. Q. Chen, Y. Q. Chen, Y.-T. Chen, B. G. Cheon, K. Chilikin, K. Chirapattpimol, H.-E. Cho, K. Cho, S.-J. Cho, S.-K. Choi, S. Choudhury, D. Cinabro, L. Corona, L. M. Cremaldi, S. Cunliffe, T. Czank, S. Das, N. Dash, F. Dattola, E. De La Cruz-Burelo, S. A. De La Motte, G. de Marino, G. De Nardo, M. De Nuccio, G. De Pietro, R. de Sangro, B. Deschamps, M. Destefanis, S. Dey, A. De Yta-Hernandez, R. Dhamija, A. Di Canto, F. Di Capua, S. Di Carlo, J. Dingfelder, Z. Doležal, I. Domínguez Jiménez, T. V. Dong, M. Dorigo, K. Dort, D. Dossett, S. Dreyer, S. Dubey, S. Duell, G. Dujany, P. Ecker, S. Eidelman, M. Eliachevitch, D. Epifanov, P. Feichtinger, T. Ferber, D. Ferlewicz, T. Fillinger, C. Finck, G. Finocchiaro, P. Fischer, K. Flood, A. Fodor, F. Forti, A. Frey, M. Friedl, B. G. Fulsom, M. Gabriel, A. Gabrielli, N. Gabyshev, E. Ganiev, M. Garcia-Hernandez, R. Garg, A. Garmash, V. Gaur, A. Gaz, U. Gebauer, A. Gellrich, J. Gemmler, T. Geßler, G. Ghevondyan, G. Giakoustidis, R. Giordano, A. Giri, A. Glazov, B. Gobbo, R. Godang, P. Goldenzweig, B. Golob, P. Gomis, G. Gong, P. Grace, W. Gradl, S. Granderath, E. Graziani, D. Greenwald, T. Gu, Y. Guan, K. Gudkova, J. Guilliams, C. Hadjivasiliou, S. Halder, K. Hara, T. Hara, O. Hartbrich, K. Hayasaka, H. Hayashii, S. Hazra, C. Hearty, M. T. Hedges, I. Heredia de la Cruz, M. Hernández Villanueva, A. Hershenhorn, T. Higuchi, E. C. Hill, H. Hirata, M. Hoek, M. Hohmann, S. Hollitt, T. Hotta, C.-L. Hsu, K. Huang, T. Humair, T. Iijima, K. Inami, G. Inguglia, N. Ipsita, J. Irakkathil Jabbar, A. Ishikawa, S. Ito, R. Itoh, M. Iwasaki, Y. Iwasaki, S. Iwata, P. Jackson, W. W. Jacobs, D. E. Jaffe, E.-J. Jang, M. Jeandron, H. B. Jeon, Q. P. Ji, S. Jia, Y. Jin, C. Joo, K. K. Joo, H. Junkerkalefeld, I. Kadenko, J. Kahn, H. Kakuno, M. Kaleta, A. B. Kaliyar, J. Kandra, K. H. Kang, S. Kang, P. Kapusta, R. Karl, G. Karyan, Y. Kato, H. Kawai, T. Kawasaki, C. Ketter, H. Kichimi, C. Kiesling, C.-H. Kim, D. Y. Kim, H. J. Kim, K.-H. Kim, K. Kim, S.-H. Kim, Y.-K. Kim, Y. Kim, T. D. Kimmel, H. Kindo, K. Kinoshita, C. Kleinwort, B. Knysh, P. Kodyš, T. Koga, S. Kohani, K. Kojima, I. Komarov, T. Konno, A. Korobov, S. Korpar, N. Kovalchuk, E. Kovalenko, R. Kowalewski, T. M. G.

Kraetzschmar, F. Krinner, P. Križan, R. Kroeger, J. F. Krohn, P. Krokovny, H. Krüger, W. Kuehn, T. Kuhr, J. Kumar, M. Kumar, R. Kumar, K. Kumara, T. Kumita, T. Kunigo, M. Künzel, S. Kurz, A. Kuzmin, P. Kvasnička, Y.-J. Kwon, S. Lacaprara, Y.-T. Lai, C. La Licata, K. Lalwani, T. Lam, L. Lanceri, J. S. Lange, M. Laurenza, K. Lautenbach, P. J. Laycock, R. Leboucher, F. R. Le Diberder, I.-S. Lee, S. C. Lee, P. Leitl, D. Levit, P. M. Lewis, C. Li, L. K. Li, S. X. Li, Y. B. Li, J. Libby, K. Lieret, J. Lin, Z. Liptak, Q. Y. Liu, Z. A. Liu, D. Liventsev, S. Longo, A. Loos, A. Lozar, P. Lu, T. Lueck, F. Luetticke, T. Luo, C. Lyu, C. MacQueen, M. Maggiora, R. Maiti, S. Maity, R. Manfredi, E. Manoni, A. Manthei, S. Marcello, C. Marinas, L. Martel, A. Martini, L. Massaccesi, M. Masuda, T. Matsuda, K. Matsuoka, D. Matvienko, J. A. McKenna, J. McNeil, F. Meggendorfer, F. Meier, M. Merola, F. Metzner, M. Milesi, C. Miller, K. Miyabayashi, H. Miyake, H. Miyata, R. Mizuk, K. Azmi, G. B. Mohanty, N. Molina-Gonzalez, S. Moneta, H. Moon, T. Moon, J. A. Mora Grimaldo, T. Morii, H.-G. Moser, M. Mrvar, F. J. Müller, Th. Muller, G. Muroyama, C. Murphy, R. Mussa, I. Nakamura, K. R. Nakamura, E. Nakano, M. Nakao, H. Nakayama, H. Nakazawa, A. Narimani Charan, M. Naruki, Z. Natkaniec, A. Natochii, L. Nayak, M. Nayak, G. Nazaryan, D. Neverov, C. Niebuhr, M. Niyyama, J. Ninkovic, N. K. Nisar, S. Nishida, K. Nishimura, M. H. A. Nouxman, K. Ogawa, S. Ogawa, S. L. Olsen, Y. Onishchuk, H. Ono, Y. Onuki, P. Oskin, F. Otani, E. R. Oxford, H. Ozaki, P. Pakhlov, G. Pakhlova, A. Paladino, T. Pang, A. Panta, E. Paoloni, S. Pardi, K. Parham, H. Park, S.-H. Park, B. Paschen, A. Passeri, A. Pathak, S. Patra, S. Paul, T. K. Pedlar, I. Peruzzi, R. Peschke, R. Pestotnik, F. Pham, M. Piccolo, L. E. Piilonen, G. Pinna Angioni, P. L. M. Podesta-Lerma, T. Podobnik, S. Pokharel, L. Polat, V. Popov, C. Praz, S. Prell, E. Prencipe, M. T. Prim, M. V. Purohit, H. Purwar, N. Rad, P. Rados, S. Raiz, A. Ramirez Morales, R. Rasheed, N. Rauls, M. Reif, S. Reiter, M. Remnev, I. Ripp-Baudot, M. Ritter, M. Ritzert, G. Rizzo, L. B. Rizzuto, S. H. Robertson, D. Rodríguez Pérez, J. M. Roney, C. Rosenfeld, A. Rostomyan, N. Rout, M. Rozanska, G. Russo, D. Sahoo, Y. Sakai, D. A. Sanders, S. Sandilya, A. Sangal, L. Santelj, P. Sartori, Y. Sato, V. Savinov, B. Scavino, M. Schnepf, M. Schram, H. Schreeck, J. Schueler, C. Schwanda, A. J. Schwartz, B. Schwenker, M. Schwickardi, Y. Seino, A. Selce, K. Senyo, I. S. Seong, J. Serrano, M. E. Sevier, C. Sfienti, V. Shebalin, C. P. Shen, H. Shibuya, T. Shillington, T. Shimasaki, J.-G. Shiu, B. Shwartz, A. Sibidanov, F. Simon, J. B. Singh, S. Skambraks, J. Skorupa, K. Smith, R. J. Sobie, A. Soffer, A. Sokolov, Y. Soloviev, E. Solovieva, S. Spataro, B. Spruck, M. Starič, S. Stefkova, Z. S. Stottler, R. Stroili, J. Strube, J. Stypula, Y. Sue, R. Sugiura, M. Sumihama, K. Sumisawa, T. Sumiyoshi, W. Sutcliffe, S. Y. Suzuki, H. Svidras, M. Tabata, M. Takahashi, M. Takizawa, U. Tamponi, S. Tanaka, K. Tanida, H. Tanigawa, N. Taniguchi, Y. Tao, P. Taras, F. Tenchini, R. Tiwary, D. Tonelli, E. Torassa, N. Toutounji, K. Trabelsi, I. Tsaklidis, T. Tsuboyama, N. Tsuzuki, M. Uchida, I. Ueda, S. Uehara, Y. Uematsu, T. Ueno, T. Uglov, K. Unger, Y. Unno, K. Uno, S. Uno, P. Urquijo, Y. Ushiroda, Y. V. Usov, S. E. Vahsen, R. van Tonder, G. S. Varner, K. E. Varvell, A. Vinokurova, L. Vitale, V. Vobbillisetti, V. Vorobyev, A. Vossen, B. Wach, E. Waheed, H. M. Wakeling, K. Wan, W. Wan Abdullah, B. Wang, C. H. Wang, E. Wang, M.-Z. Wang, X. L. Wang, A. Warburton, M. Watanabe, S. Watanuki, J. Webb, S. Wehle, M. Welsch, C. Wessel, J. Wiechczynski, P. Wieduwilt, H. Windel, E. Won, L. J. Wu, X. P. Xu, B. D. Yabsley, S. Yamada, W. Yan, S. B. Yang, H. Ye,

J. Yelton, J. H. Yin, M. Yonenaga, Y. M. Yook, K. Yoshihara, T. Yoshinobu, C. Z. Yuan, Y. Yusa, L. Zani, Y. Zhai, J. Z. Zhang, Y. Zhang, Y. Zhang, Z. Zhang, V. Zhilich, J. Zhou, Q. D. Zhou, X. Y. Zhou, V. I. Zhukova, V. Zhulanov, R. Žlebčík

Abstract

We report the measurement of the branching fraction of the $B^0 \rightarrow K_s^0 \pi^0 \gamma$ decay in $e^+ e^- \rightarrow \Upsilon(4S) \rightarrow B\bar{B}$ data recorded by the Belle II experiment at the SuperKEKB asymmetric-energy collider and corresponding to 190 fb^{-1} of integrated luminosity. The signal yield is measured to be $121 \pm 29 \text{ (stat)}$, leading to the branching fraction $\mathcal{B}(B^0 \rightarrow K_s^0 \pi^0 \gamma) = (7.3 \pm 1.8 \text{ (stat)} \pm 1.0 \text{ (syst)}) \times 10^{-6}$, which agrees with the known value.

1. INTRODUCTION

In the Standard Model (SM), $b \rightarrow s\gamma$ transitions are forbidden at tree level and are possible only through a quantum loop. Due to the chiral structure of the SM, the radiated photon in $b \rightarrow s\gamma$ transitions is predominantly left-handed for b and right-handed for \bar{b} quarks. This makes $B^0\bar{B}^0$ interference in such decays less probable and leads to a suppression, proportional to the s quark mass over the b quark mass, of the decay-time-dependent CP -violating asymmetry between B^0 and \bar{B}^0 decay rates. A broad class of non-SM physics scenarios [1] feature a different chiral structure and thus may lead to deviations from the SM expectation by introducing different photon polarizations in the transition. These non-SM models can be probed via measurements of time-dependent CP asymmetry (TDCPV) parameters at B -Factories.

The $b \rightarrow s\gamma$ process with the highest branching fraction is the $B^0 \rightarrow K_s^0\pi^0\gamma$ decay, which is produced through the $K^{*0}(892)$ resonance and higher-mass kaonic resonances, such as $K_1^0(1270)$ and $K^{*0}(1410)$, often denoted as X_{sd} . Previous TDCPV measurements with this channel have been reported by the Belle and BaBar collaborations [2, 3]. They do not depart from the SM prediction. However their precision is still limited by the small signal sample sizes, which motivates further exploration of the $b \rightarrow s\gamma$ transitions using the large data set expected from the Belle II experiment at the SuperKEKB collider.

The latest Belle II branching fraction measurement of $B \rightarrow K^*\gamma$ [4] was based on 63 fb^{-1} and was optimised to measure the CP -violating parameter A_{CP} and the isospin violating-parameter Δ_{0+} when Belle II will accumulate more data. In this paper, we report the measurement of the branching fraction of the $B^0 \rightarrow K_s^0\pi^0\gamma$ decay channel (and its charge conjugate) with decays restricted to those with $K_s^0\pi^0$ mass smaller than $1.1 \text{ GeV}/c^2$ corresponding to the region dominated by the K^{*0} resonance, as a forerunner of the full TDCPV analysis. The analysis uses 190 fb^{-1} of data, corresponding to the luminosity integrated by Belle II available by winter 2021.

The outline of this paper is as follows. A description of the Belle II detector and the data set used is given in Section 2. In Section 3, the candidate reconstruction, the selection and the yield extraction method are explained. The result of the measurement of the branching fraction is given in Section 4 and all source of systematic uncertainties are detailed. Finally, the result is summarized in Section 5.

2. THE BELLE II DETECTOR AND DATA SET

The Belle II experiment [5] operates at the SuperKEKB asymmetric-energy electron-positron collider [6], located at the KEK laboratory in Tsukuba, Japan. It consists of various subsystems. The innermost subsystem is the vertex detector, which includes two layers of silicon pixel detectors and four outer layers of silicon strip detectors. Currently, the second pixel layer covers approximately only 15% of the azimuthal range, while the remaining vertex detector layers are fully installed. Most of the tracking volume is occupied by a helium and ethane-based small-cell drift chamber (CDC). Outside the drift chamber, a Cherenkov-light imaging and time-of-propagation detector provides charged-particle identification in the barrel region. In the forward endcap, this function is provided by a proximity-focusing, ring-imaging Cherenkov detector with an aerogel radiator. Further out is the electromagnetic calorimeter (ECL), consisting of a barrel and two endcap sections made of CsI(Tl) crystals. A uniform 1.5 T magnetic field is provided by a supercon-

ducting solenoid situated outside the calorimeter. Multiple layers of scintillators and resistive plate chambers, located between the magnetic flux-return iron plates, constitute the K_L^0 and muon identification system. The z axis of the laboratory frame is defined as the symmetry axis of the solenoid, pointing approximately at the incoming electron beam.

The data used in this analysis were collected between March 2019 and July 2021. They correspond to a total integrated luminosity of 190 fb^{-1} obtained at the center-of-mass energies at or near the $\Upsilon(4S)$ resonance (10.58 GeV). The sample corresponds to $N_{B\bar{B}} = (197 \pm 6) \times 10^6$ $B^0\bar{B}^0$ and B^+B^- events determined following Ref. [7]. To optimize the analysis procedure and determine the detection and selection efficiency, two sets of events simulated using Monte Carlo (MC) are used. The first simulation sample, hereafter referred to as the signal MC sample, contains two million $B^0\bar{B}^0$ events where one of the B is forced to decay in the signal decay channel. A second sample equivalent to an integrated luminosity of 700 fb^{-1} , referred as generic MC, combines all possible event types $e^+e^- \rightarrow B^0\bar{B}^0$, B^+B^- , $u\bar{u}$, $d\bar{d}$, $c\bar{c}$ and $s\bar{s}$. The signal and $e^+e^- \rightarrow \Upsilon(4S) \rightarrow B\bar{B}$ samples are generated using the EvtGen package [8], while the continuum background events are generated with the KKMC [9] generator interfaced with Pythia [10]; the detector response is then simulated by the Geant4 package [11].

Both data and simulated data sets are analysed with Belle II analysis software framework, **basf2** [12].

3. ANALYSIS

3.1. Candidate reconstruction and selection

We search for candidate B^0 decays with five or more charged particles in the event, at least one energy deposit (cluster) in the ECL larger than 0.2 GeV, and at least 4 GeV of visible energy in the center-of-mass frame to enrich the sample in events with high-energy photons. We reconstruct K_s^0 candidates from the association of two oppositely charged particles within the CDC acceptance and originating from the interaction point. For these particles, the distance of closest approach to the e^+e^- interaction point is required to be smaller than 2.0 cm in the plane transverse to the z axis and smaller than 4.0 cm along the z axis. The K_s^0 properties are obtained from a kinematic fit of the trajectories of both charged particles (tracks) assumed to be pions. Events with K_s^0 candidates with mass outside the range 0.450 to 0.550 GeV/c^2 are discarded. We reconstruct π^0 candidates from the combination of two photons, each having an energy of at least 30 MeV in the barrel, 80 MeV in the forward endcap or 60 MeV in the backward endcap of the ECL. Only pairs with an invariant mass within 0.120 to 0.145 GeV/c^2 are kept. High-energy photons are selected if their energy in the laboratory frame is comprised between 1.4 and 4.0 GeV. With a π^0 and η veto, consisting in a boosted decision-tree (BDT) trained on event-based variables, we reject photons consistent with products of π^0 and η diphoton decays with 70% probability or more.

Finally, the reconstructed B^0 candidates combine one K_s^0 , one π^0 and one high-energy photon in a kinematic fit including a pointing constraint to the interaction point [13]. Then we construct two variables based on the center-of-mass energy of the collisions, \sqrt{s} , the B invariant mass constrained by the beam energy $m_{bc} = \sqrt{(\sqrt{s}/2)^2 - p_B^{*2}}$ and the energy difference $\Delta E = E_B^* - \sqrt{s}/2$, where p_B^* and E_B^* are respectively the B^0 candidate momentum

and energy in the center-of-mass frame. We require that $5.20 < m_{bc} < 5.29 \text{ GeV}/c^2$ and $-0.5 < \Delta E < 0.5 \text{ GeV}$.

This first reconstruction and selection step retains approximately 28% of the signal decay. The signal significance, $S/\sqrt{S+B}$ where S and B are respectively the number of signal decays and background events from simulation, is still too low and further selection requirements are needed. Additional variables are considered: a threshold of 36 for the K_s^0 decay length significance, computed from the ratio of the decay length over its uncertainty, is used to suppress background in the K_s^0 sample; a maximal value of $1.1 \text{ GeV}/c^2$ for the $M(K_s^0\pi^0)$ mass allows to retain most of the K^{*0} decays and reject the ones from the X_{sd} resonances; a threshold of $5.275 \text{ GeV}/c^2$ is required on the beam-constrained mass m_{bc} ; finally, to suppress the dominant background originating from continuum events $e^+e^- \rightarrow q\bar{q}$, we combine thirty event-shape variables and kinematic properties of the event into a binary BDT classifier [14] trained over 60000 signal events and an equal amount of simulated background events. These four selection criteria values are optimized to maximize the significance over the 700 fb^{-1} generic MC data sample. After this selection, for events containing multiple candidates, the one featuring the lowest χ^2 from the B^0 vertex fit is chosen and all others discarded. There is only one candidate on more than half of the event and the efficiency to select the correctly reconstructed signal from an event with multiple reconstructed B candidates is 87%.

The efficiency is then corrected from the discrepancies observed between data and simulation described in Section 4.2. The final total selection efficiency reaches $\epsilon = (8.7 \pm 0.7)\%$, where the quoted uncertainty comes from the total systematic uncertainty from Table I.

3.2. Yield extraction

The signal yield is extracted from an extended maximum likelihood fit to the ΔE distribution, where the total probability density function includes two contributions, one for the signal and the other for the background. A single Chebyshev polynomial of order two is used to model the background contribution. The two parameters a_0 and a_1 are fixed from a fit to the 700 fb^{-1} generic MC sample, shown in Figure 1. A Johnson distribution [15], which acts like a double-sided Crystal Ball function [16], describes the signal contribution with four parameters, one associated with the location of the peak, and three with the shape. The parametrization of the Johnson distribution reads

$$\text{PDF}_{\text{Johnson}}(\Delta E; \mu, \sigma, \lambda, \gamma) = \frac{\lambda}{\sigma\sqrt{2\pi}} \frac{1}{\sqrt{1 + \left(\frac{\Delta E - \mu}{\sigma}\right)^2}} \exp\left[-\frac{1}{2} \left(\gamma + \lambda \operatorname{arsinh}\left(\frac{\Delta E - \mu}{\sigma}\right)\right)^2\right], \quad (1)$$

where μ and σ , which drive the central value and width of the distribution, are determined by the fit and the parameters λ and γ are fixed from a fit to the signal MC sample (see Figure 1). The third (and last) floating parameter in the fit is the signal yield.

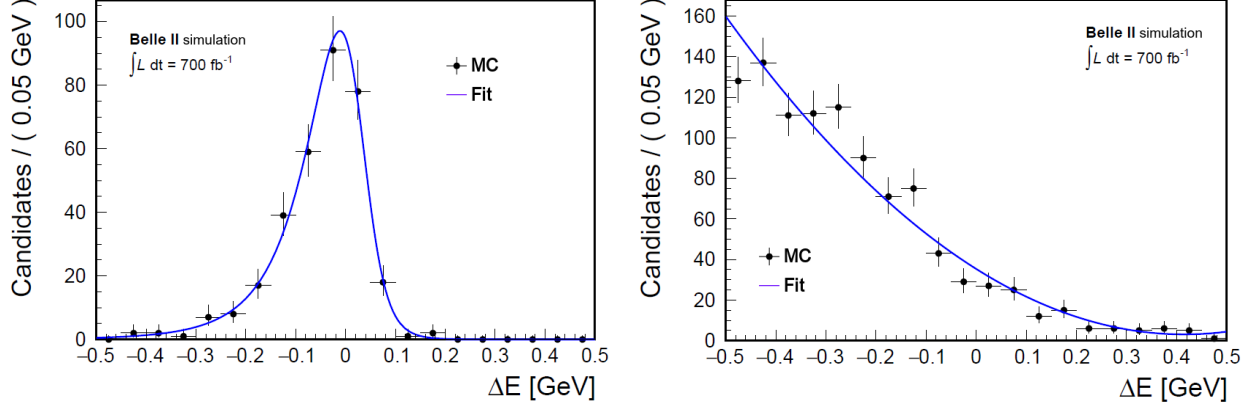


FIG. 1: Distribution of ΔE for candidates selected in simulated samples corresponding to 700 fb^{-1} of (left) signal $B^0 \rightarrow K_s^0\pi^0\gamma$ decays and (right) $e^+e^- \rightarrow \Upsilon(4S)$ events with modeling-fit projections overlaid.

4. RESULTS AND SYSTEMATIC UNCERTAINTIES

4.1. Measurements of the branching fraction

The fit described in Section 3.2 is applied to the ΔE distribution of the selected candidates. Figure 2 depicts the data and the fitted function overlaid. The observed $B^0 \rightarrow K_s^0\pi^0\gamma$ yield is $N_{\text{yield}} = 121 \pm 29 \text{ (stat)}$.

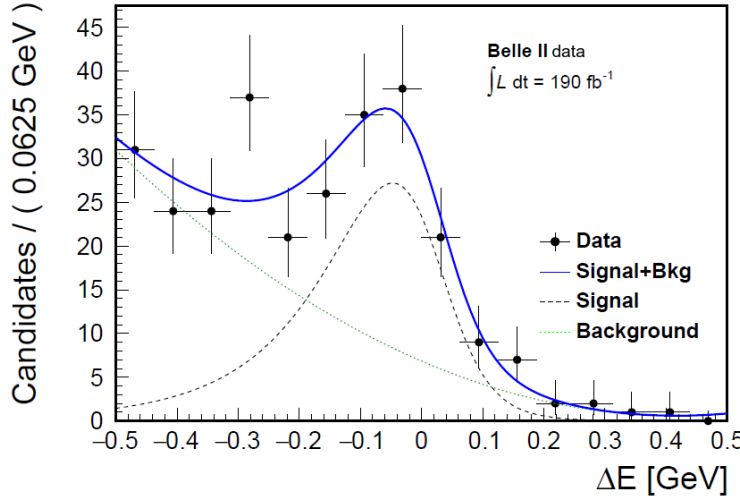


FIG. 2: Distribution of ΔE for candidates selected in data sample corresponding to 190 fb^{-1} of $B^0 \rightarrow K_s^0\pi^0\gamma$ decays with modeling-fit projections overlaid.

The branching fraction is computed from

$$\mathcal{B} = \frac{N_{\text{yield}}}{2\epsilon f^{00} N_{B\bar{B}}}, \quad (2)$$

where ϵ is the overall detection and selection efficiency for the $B^0 \rightarrow K_s^0 \pi^0 \gamma$ decay estimated in Section 3.1, $f^{00} = (48.6 \pm 0.6)\%$ [17] is the branching fraction of $\Upsilon(4S)$ going to $B^0 \bar{B}^0$, and $N_{B\bar{B}}$ is the quoted number of $B\bar{B}$ pairs produced in the data sample listed in Section 2 [7]. We find the following branching fraction

$$\mathcal{B}(B^0 \rightarrow K_s^0 \pi^0 \gamma) = (7.3 \pm 1.8 \text{ (stat)}) \times 10^{-6}. \quad (3)$$

4.2. Systematic uncertainties

Systematic uncertainties arising from the generation, reconstruction, selection, fit and yield extraction procedures are considered and discussed below. All relative systematic uncertainty values are summarized in Table I. A systematic uncertainty of 0.2% is assigned due to the finite sample size of the MC signal sample. To assign the systematic uncertainty related to the model of the K^{*0} resonance, we check the efficiencies of the $M(K_s^0 \pi^0)$ restriction after the preselection and reconstruction and after the whole selection except for this criterion. We assign a relative systematic uncertainty of 2.0% to the efficiency. For the π^0 selection, the difference in reconstruction efficiency between data and simulation is estimated by comparing the $\eta \rightarrow \gamma\gamma$ and $\eta \rightarrow \pi^0 \pi^0 \pi^0$ yields. A relative uncertainty of 5.5% is assigned. Comparing the reconstruction efficiency of K_s^0 between data and simulation, a systematic uncertainty of 3.5% and a correction factor of 0.9654 is assigned to the efficiency. The systematic uncertainty related to the π^0 and η veto is evaluated by comparing the efficiency of that veto between real and simulated $B^0 \rightarrow D^- \pi^+$ and $B^+ \rightarrow \bar{D}^0 \pi^+$ samples. The efficiency is extracted as a function of the photon energy. We assign a systematic uncertainty of 1.9% and a correction factor of 1.034 on the efficiency. According to the measurement of the data to MC ratio of photon reconstruction efficiency in the calorimeter, using radiative muon pair events, we assign a relative uncertainty of 0.3% for the photon selection. The systematic uncertainty due to the discrepancies between data and simulation of the efficiency associated with the BDT selection in the off-resonance data, recorded 60 MeV below $\Upsilon(4S)$ resonance, is evaluated to be 3.0%. To check the estimator properties, we perform a MC study: 500 data sets, each corresponding to an integrated luminosity of 200 fb^{-1} , are created by bootstrapping the initial 700 fb^{-1} MC sample. Then the final fit procedure is performed for each data set. We observe an overestimation in the signal yield. We tried to reduce this bias by testing different fitting function or fitting the peaking $B^+ B^-$ background around -0.3 GeV, but no improvements were observed. We assign a systematic uncertainty of 11.5%. A systematic uncertainty of 2.9% is assigned due to the uncertainty in the number of produced $B\bar{B}$ pairs. A systematic uncertainty of 1.2% is assigned due to the uncertainty in the branching fraction of $\Upsilon(4S)$ decaying to $B\bar{B}$ from Ref. [17].

TABLE I: Summary of systematic uncertainties considered for the measurement of the $B^0 \rightarrow K_s^0 \pi^0 \gamma$ branching fraction. The total efficiency systematic corresponds to the quadratic sum of all the systematic uncertainties for the selection efficiency.

MC sample size	0.2%
MC generation	2.0%
π^0 reconstruction	5.5%
K_s^0 reconstruction	3.5%
$\pi^0\eta$ veto	1.9%
γ selection	0.3%
Continuum suppression	3.0%
Total efficiency	7.7%
Fit bias	11.5%
Number of $B^0\bar{B}^0$ pairs	2.9%
f^{00} systematic	1.2%
Total systematic on \mathcal{B}	14.2%

5. CONCLUSION

Using a sample of data corresponding to 190 fb^{-1} recorded with the Belle II experiment, we report a measurement of the branching fraction for the $B^0 \rightarrow K_s^0 \pi^0 \gamma$ decay with a larger sample size than reported in Ref. [4]. The measured branching fraction for this decay is

$$\mathcal{B}(B^0 \rightarrow K_s^0 \pi^0 \gamma) = (7.3 \pm 1.8 \text{ (stat)} \pm 1.0 \text{ (syst)}) \times 10^{-6}, \quad (4)$$

which is compatible with the known value of $(7.0 \pm 0.4) \times 10^{-6}$ [17].

6. ACKNOWLEDGMENTS

We thank the SuperKEKB group for the excellent operation of the accelerator; the KEK cryogenics group for the efficient operation of the solenoid and the KEK computer group for on-site computing support.

- [1] D. Atwood, M. Gronau, and A. Soni, *Mixing-Induced CP Asymmetries in Radiative B Decays in and beyond the Standard Model*, Phys. Rev. Lett. **79** (1997) 185–188, [arXiv:9704272 \[hep-ph\]](https://arxiv.org/abs/9704272).
- [2] Y. Ushiroda et al., Belle collaboration, *Time-Dependent CP Asymmetries in $B^0 \rightarrow K_S^0 \pi^0 \gamma$ transitions*, Phys. Rev. **D74** (2006) 111104, [arXiv:hep-ex/0608017 \[hep-ex\]](https://arxiv.org/abs/hep-ex/0608017).
- [3] B. Aubert et al., BaBar collaboration, *Measurement of Time-Dependent CP Asymmetry in $B^0 \rightarrow K_S^0 \pi^0 \gamma$ Decays*, Phys. Rev. **D78** (2008) 071102, [arXiv:0807.3103 \[hep-ex\]](https://arxiv.org/abs/0807.3103).
- [4] F. Abudinén et al., Belle II collaboration, *Measurements of the branching fractions for $B \rightarrow K^* \gamma$ decays at Belle II*, [arXiv:2110.08219 \[hep-ex\]](https://arxiv.org/abs/2110.08219).

- [5] T. Abe et al., Belle II collaboration, *Belle II Technical Design Report*, [arXiv:1011.0352 \[physics.ins-det\]](https://arxiv.org/abs/1011.0352).
- [6] K. Akai, K. Furukawa, and H. Koiso, SuperKEKB, *SuperKEKB Collider*, Nucl. Instrum. Meth. A **907** (2018) 188–199, [arXiv:1809.01958 \[physics.acc-ph\]](https://arxiv.org/abs/1809.01958).
- [7] C. Cecchi et al., Belle II collaboration, *B counting measurement in "Moriond 2022" Belle II dataset*, BELLE2-NOTE-PH-2022-007 (2022) . <https://docs.belle2.org/record/2846/>.
- [8] D. J. Lange, *The EvtGen particle decay simulation package*, Nucl. Instrum. Meth. A **462** (2001) 152–155.
- [9] B. F. L. Ward, S. Jadach, and Z. Was, *Precision calculation for $e+ e^- \rightarrow 2f$: The KK MC project*, Nucl. Phys. B Proc. Suppl. **116** (2003) 73–77, [arXiv:hep-ph/0211132](https://arxiv.org/abs/hep-ph/0211132).
- [10] T. Sjostrand et al., *A brief introduction to PYTHIA 8.1*, Comp. Phys. Comm. **178** (2008) 852–867.
- [11] S. Agostinelli et al., GEANT4, *GEANT4—a simulation toolkit*, Nucl. Instrum. Meth. A **506** (2003) 250–303.
- [12] T. Kuhr et al., Belle II collaboration, *The Belle II Core Software*, Comput. Softw. Big. Sci. **3** (2018) , [arXiv:1809.04299 \[physics.comp-ph\]](https://arxiv.org/abs/1809.04299).
- [13] J.-F. Krohn et al., Belle II collaboration, *Global decay chain vertex fitting at Belle II*, Nucl. Instrum. Meth. A**976** (2020) 164269, [arXiv:1901.11198 \[hep-ex\]](https://arxiv.org/abs/1901.11198).
- [14] A. Bevan et al., *The Physics of the B Factories*, Eur. Phys. J. **C74** (2014) 3026.
- [15] N. L. Johnson, *Systems of Frequency Curves Generated by Methods of Translation*, Biometrika **36** (1949) 149–176.
- [16] T. Skwarnicki, *A study of the radiative CASCADE transitions between the Upsilon-Prime and Upsilon resonances*. PhD thesis, Cracow, INP, 1986.
<https://inspirehep.net/literature/230779>.
- [17] P. Zyla and others. (Particle Data Group), *Review of Particle Physics*, Prog. Theor. Exp. Phys. **2020** (2020) no. 8, 071102. 083C01.